

# Seoul National University Bright Quasar Survey in Optical (SNUQSO) II: Discovery of 40 Bright Quasars near the Galactic Plane

Myungshin Im<sup>1,2</sup>, Induk Lee<sup>1,3</sup>, Yunseok Cho<sup>1</sup>, Changsu Choi<sup>1</sup>, Jongwan Ko<sup>1</sup>, and Mimi Song<sup>1</sup>

## ABSTRACT

We report the discovery of 40 bright quasars and active galactic nuclei (AGNs) at low Galactic latitude ( $b < |20^\circ|$ ). The low galactic latitude region has been considered as a place to avoid when searching for extragalactic sources, because of the high Galactic extinction as well as a large number of stars contaminating the sample selection. Bright quasars ( $R \lesssim 17$ ) suffer more from such difficulties because they look like bright stars, which are numerous at low  $b$ , yet their surface number density is very low. In order to find quasars in this region of the sky less explored for extragalactic sources, we have started a survey of low Galactic latitude bright quasars as a part of the Seoul National University Quasar Survey in Optical (SNUQSO). Quasar candidates have been selected from radio and near-infrared (NIR) data. Out of 88 targets, we identify 29 bright quasars/AGNs around the antigalactic center, and 11 bright quasars/AGNs in the outskirts of the Galactic center, from two observing runs in 2006 at the Bohyunsan Optical Astronomical Observatory (BOAO) in Korea. Our finding demonstrates that quasars/AGNs can be discovered effectively even at low Galactic latitude using multi-wavelength data.

*Subject headings:* quasars: general — galaxies: active — techniques: spectroscopic — surveys

---

<sup>1</sup>Astronomy Program, Department of Physics and Astronomy, FPRD, Seoul National University, Seoul, Korea

<sup>2</sup>mim@astro.snu.ac.kr

<sup>3</sup>idlee@astro.snu.ac.kr

## 1. INTRODUCTION

Since the discovery of quasar 3C273 in 1963 (Schmidt 1963), more than 100,000 quasars and active galactic nuclei have been found to date (Schneider et al. 2005; Croom et al. 2004; Hagen et al. 1995; Hewett et al. 1995; Becker et al. 2001; Schmidt & Green 1983; Veron-Cetty & Veron 2006). Despite of the rapid increase in the number of known quasars, however, only a small number of quasars have been discovered near the Galactic plane. The dots and crosses in Figure. 1 represent the positions of quasars discovered to date, taken from Veron-Cetty & Veron (2006). Clearly, there is a lack of quasars/AGNs at low Galactic latitude ( $b \lesssim |20|$ ). There are two reasons for this paucity of quasars at low Galactic latitude. First, there are simply too many stars that look like quasars at low Galactic latitude so that it is much more challenging to select quasar candidates in such a region than at a high Galactic latitude region. High Galactic extinction in the Galactic plane also causes a trouble when searching for quasars. Not only does Galactic extinction dim the light from quasars by several magnitudes or more, but it also affects the optical colors of quasars, making it difficult to isolate quasar candidates with otherwise highly efficient quasar selection methods employing optical color-color diagrams (e.g., Richards et al. 2004).

Among quasars, bright quasars ( $V \lesssim 17$  mag) get special attention. Because of their brightness, they are easy to use to investigate the intergalactic medium (e.g., Weymann et al. 1981; Rauch 1998; Fan et al. 2006), the properties of supermassive blackholes and their host galaxies (e.g., Kaspi et al. 2000; Kim et al. 2006), and the physical state and distribution of gas in our Galaxy (Sternberg 2003; Sembach et al. 2003; Savage & Sembach 1996). Because of their usefulness, bright quasars have been searched for extensively in high Galactic latitude regions, especially in the northern hemisphere (Schmidt & Green 1983; Hagen et al. 1995; Hewett et al. 1995; Becker et al. 2001; Schneider et al. 2005). These surveys appear to have found the majority of bright quasars in their respective search areas, although a small number of bright quasars are still waiting to be discovered (Lee et al. 2008).

Bright quasars at low Galactic latitude also have many astrophysical applications. They can allow us to study the gaseous component of matter in our galaxy from a unique point of view through their absorption lines, and offer an opportunity to study their host galaxies using bright stars close to them as guide stars for adaptive optics. They can also serve as reference points to examine the motion of stars in our Galaxy. However, finding bright quasars at low Galactic latitude seems to be a daunting job considering the aforementioned difficulties. A simple quantitative argument is given below to demonstrate how difficult it is to identify bright quasars at low Galactic latitude. The surface number density of bright quasars at  $V < 17$  mag is  $0.1 \text{ deg}^{-2}$ , while the number density of stars at low Galactic latitude ranges from a few thousand (anti-galactic center) to a few tens of thousand per

square degree at around  $l = 0^\circ$  and  $b = 10^\circ$  (Robin et al.2003). This is 10 to 100 times more than the number density of stars at high Galactic latitude (Spagna et al. 1996). These numbers become even worse if we take into account Galactic extinction which dims the light from extragalactic objects by more than a magnitude in most areas at low Galactic latitude. Assuming 1 magnitude extinction, the apparent magnitude cut of  $V < 17$  mag at low Galactic latitude would actually sample quasars with  $V < 16$  mag if they were at high Galactic latitude. At  $V < 17$  mag, the number density of quasars is only  $0.01 \text{ deg}^{-2}$ . Therefore, the quasar-to-star ratio of an apparent magnitude-limited sample at  $V < 17$  mag becomes 1 in a few hundred thousand to a few million, or 100 to 1000 times worse than at high Galactic latitude. At  $V \lesssim 17$ , the optical multi-color selection gives a quasar identification efficiency of about 90%, but at low Galactic latitude this efficiency would drop to 9% to 0.9% following the above argument. Clearly an alternative method is needed for selecting bright quasars at low Galactic latitude.

In order to broaden our knowledge of bright quasars toward the zone of avoidance, we have started a survey of bright quasars at low Galactic latitude regions, as a part of the Seoul National University Quasar Survey in Optical (SNUQSO). Here, we report the discovery of 40 bright quasars/AGNs at low Galactic latitude, using a selection algorithm designed to efficiently sample low Galactic latitude quasars. Throughout the paper, the magnitudes are Vega-based, unless otherwise mentioned. Also, we adopt the cosmological parameters of  $\Omega_m = 0.3$ ,  $\Lambda = 0.7$ , and  $H_0 = 70 \text{ km s}^{-1} \text{ Mpc}^{-1}$ .

## 2. SELECTION OF CANDIDATES

### 2.1. Method

The key to successfully finding low Galactic latitude quasars lies in an efficient algorithm that can distinguish quasars from the plethora of stars and dust in the Galactic plane. To achieve such a goal, we use a combination of radio and near-infrared (NIR) data. For the radio data, we use the NRAO VLA Sky Survey (NVSS; Condon et al. 1998) data set, and for the NIR data, we use the Two Micron All Sky Survey (2MASS) data set (Skrutskie et al. 2006). These data sets are chosen because they provide nearly complete coverage of the Galactic plane to the depth sufficient for finding a fair number of bright quasars. The NVSS data covers the whole sky above  $\delta = -40^\circ$  to the depth of 2.5 mJy in 21cm. The 2MASS data covers the entire sky to the depth of  $K = 15$  mag. The reason for the use of the radio and NIR data sets is elaborated below.

Our selection of candidates starts with identifying radio sources at  $|b| < 20$ . As the name

“quasar” originates from the word “quasi-stellar radio star,” it has been widely recognized that radio emitting point sources are very likely to be quasars or AGNs. The usual procedure for finding quasars using radio data is to find an optical counterpart to the radio source and perform spectroscopic observation to determine whether it is a quasar. In high Galactic latitude regions, it is not very difficult to identify the optical counterpart of a radio source, given that the radio data have a reasonably good positional accuracy. For example, the FIRST survey data show that the matching radius of  $1''$  is sufficiently good for finding an optical counterpart (White et al. 2000). However, that approach is not directly applicable in this case. The beam size of the NVSS data is large (FWHM =  $45''$ ) compared to FIRST, and the quoted positional accuracy of point sources varies from  $rms \sim 1''$  (for sources brighter than 15 mJy) to  $7''$  (at the survey limit of 2.5 mJy), forcing us to adopt a conservative  $2\text{-}\sigma$  radius of  $15''$  as a search radius to identify the optical counterpart. However, within a  $15''$  radius circle of a NVSS radio source at low Galactic latitude, there are on average  $\sim 6$  point sources down to the optical magnitude of  $R \lesssim 19$  mag and sometimes more.

In order to improve the quasar selection efficiency by weeding out stars near the radio position, we add a NIR selection method. Low redshift quasars are known to have red  $J - K$  colors due to a steeply rising NIR spectra (e.g., Glikman et al. 2006), and NIR colors have been used previously to select quasars and AGNs (e.g., Figure 5 in Barkhouse & Hall 2001; see also, Nelson et al. 1998; Cutri et al. 2000; Maddox & Hewett 2006). Therefore, we applied a NIR color cut on point sources near the radio position and selected objects with  $J - K > 1.4$  as quasar candidates. The NIR cut of  $J - K > 1.4$  has been found to be the optimal cut for minimizing the contamination from stars and galaxies by performing the above selection method on known quasars/galaxies/stars in the fourth data release of the Sloan Digital Sky Survey (SDSS; Adelman-McCarthy, et al. 2006). In general, the selected candidates have  $K < 14$  mag and an optical magnitude of  $R < 19$ . With the NIR cut, the contamination rate of stars/galaxies on the SDSS sample with the above method is found to be on the order of a few percent or less, but at the expense of preferentially selecting low redshift quasars at  $z \lesssim 0.4$  (see also, Chiu et al. 2007). A more complete description of the sample selection and its efficiency will appear in I. Lee et al. (2008, in preparation).

Although our method can be applied to a very crowded region in the Galactic plane, we have limited the initial survey area to the following region so that we get a reasonably high quasar identification efficiency of  $\sim 50\%$ .

$$\begin{aligned}
 |b| < 20^\circ & \quad \text{at } 120^\circ < l < 240^\circ \\
 5^\circ < |b| < 20^\circ & \quad \text{at } 40^\circ < l < 120^\circ \ \& \ 240^\circ < l < 320^\circ \\
 10^\circ < |b| < 20^\circ & \quad \text{at } 0^\circ < l < 40^\circ \ \& \ 320^\circ < l < 360^\circ
 \end{aligned}$$

Using this selection method, we identify 601 candidates in the above area covering  $10919.9 \text{ deg}^2$ , 88 of which were observed over  $\sim 2700 \text{ deg}^2$  during 2006, as described in the next section.

### 3. OBSERVATION

For spectroscopic confirmation of quasars, we observed the quasar candidates using the longslit low-resolution spectrograph mounted on the Bohyunsan Observatory Eschelle Spectrograph (BOES) of the 1.8m telescope at Bohyunsan Optical Astronomical Observatory (BOAO; Kim et al. 2003). The spectroscopic observations were carried out on 2006 June 17 - 24 and 2006 December 20 - 25, among which about four nights were in observable condition under the seeing of  $2 - 3''$ . Using a 150 per mm grating and a slit width of  $3.6''$ , we covered the wavelength range of  $4200 - 8400 \text{ \AA}$  at the spectral resolution of  $\lambda/\delta\lambda \sim 366$ , or  $\delta v \sim 820 \text{ km s}^{-1}$ . The observational setting is basically identical to the default observational setting of SNUQSO, which is described in more detail in Lee et al. (2008). The June run targeted bright quasar candidates in the outskirts of the Galactic center, while in the December run, we observed targets near the anti-galactic center. We observed 33 candidates in June, and 55 candidates in December. The observed data were reduced with IRAF<sup>1</sup> packages, following a standard procedure including flux calibration. We estimate the accuracy of the relative flux calibration (as a function of wavelength) to be roughly 15% (Lee et al. 2007a). We originally took optical magnitudes from the USNO-A2.0 catalog (Monet et al. 1998) for the quasar candidates, but some of the apparent magnitudes appeared to be too bright. In order to check the USNO magnitudes, we performed the multi-band imaging observation of objects that are identified as quasars/AGNs using the 1.5m telescope at the Mt. Maidanak Observatory in Uzbekistan during 2006 August 1 - 12 and also in 2006 June/July (M. Im et al. 2008, in preparation). The median seeing during the imaging run hovered around  $0.7''$  to  $1.0''$ , and the observations were carried out in photometric condition. Our imaging observation reveals that the USNO magnitudes are too bright by more than 1 mag for the four objects with USNO magnitude  $R < 15$  (object numbers, 33, 36, 37, and 39 in Table 1), and we have revised the  $R$ -band and  $B$ -band magnitude accordingly. In other cases, we find that the average difference in  $R$ -band magnitude is  $R(\text{USNO}) - R(\text{Maidanak}) \simeq 0.12$  mag. Table 1 lists the apparent magnitudes of the low Galactic latitude quasars/AGNs. The  $R$ -band and  $B$ -band magnitude of objects 29-39 in Table 1 are from our imaging observation,

---

<sup>1</sup>IRAF is distributed by the National Optical Astronomy Observatory, which is operated by the Association of Universities for Research in Astronomy, Inc., under cooperative agreement with the National Science Foundation.

while the rest come from the USNO catalog. For some of the problematic cases, the blending of objects might be responsible for the bright USNO magnitude since we find neighbors within  $\sim 6''$  of the quasar. For the rest, it is not clear why the USNO magnitudes are so bright. Monitoring of the quasars/AGNs may reveal the temporal variation of brightness of such quasars/AGNs. Based on our imaging data of 11 objects, we note that the magnitudes in Table 2 originating from the USNO catalog may be too bright when  $R < 15$  mag.

#### 4. RESULTS AND DISCUSSIONS

From the observed spectra, quasars were identified as objects with redshifted, broad Balmer emission lines with their FWHM line widths exceeding  $1000 \text{ km s}^{-1}$  (White et al. 2000; Schneider et al. 2003). With such a criterion, we find 40 quasars among 88 candidates. Application of an absolute magnitude cut of  $M_i < -22$  AB magnitude (Schneider et al. 2003) reduces this number to 37<sup>2</sup>

Figure 1 shows the distribution of the 40 new quasars/AGNs in Galactic coordinates (triangles and squares). Also plotted in the figure are quasars and active galaxies listed in Veron-Cetty & Veron (2006). We also plot quasars brighter than  $V = 17$  mag as crosses. The lack of bright quasars at low Galactic latitude is apparent from this figure. Especially in the Galactic plane near the anti-galactic center ( $120^\circ < l < 240^\circ$  and  $|b| < 8^\circ$ ), only 7 bright quasars/AGNs have been reported previously. We more than double this number now by discovering 13 additional quasars/AGNs in this region.

In Figure 2, we present the spectra of the 40 quasars/AGNs, while Table 1 summarizes the basic observed properties of these quasars. The extinction corrected absolute  $R$ -band magnitude,  $M_R$ , is calculated with the formula,

$$M_R = m_R - 5 \times \log(d_L(z)) - 25 - K_R(z) - A_R.$$

Here,  $m_R$  is the  $R$ -band apparent magnitude before extinction correction (col. [8] in Table 1),  $d_L$  is the luminosity distance,  $K_R(z)$  is the  $K$ -correction,<sup>3</sup> derived from the composite spectrum of SDSS quasars (Vanden Berk et al. 2001), and  $A_R$  is the Galactic extinction

---

<sup>2</sup> $M_i$  can be calculated from the  $R$ -band absolute magnitude listed in Table 1, by applying the color correction of  $R(\text{Vega}) - i_{AB} \simeq -0.1$  mag, which we derived using a template quasar spectrum from Vanden Berk et al. (2001). Here,  $R(\text{Vega}) - i_{AB}$  would be  $\sim -0.2$  mag for the  $R$ -band magnitudes from USNO based on the comparison of the USNO  $R$ -band magnitude to our data.

<sup>3</sup>Note that the correction is calculated assuming the Bessel  $R$ -band filter response on the 4k x 4k CCD

toward the position of the quasar/AGN taken from NASA/IPAC Extragalactic Database, which is based on the reddening map of Schlegel et al. (1998). Figure 2 shows a clear detection of redshifted  $H\alpha$ ,  $H\beta$ , and  $[OIII]$  lines. Redshifts of these quasars/AGNs range from  $z = 0.05$  to  $0.3$ , and the rest-frame FWHMs are all measured to be well above  $1000 \text{ km s}^{-1}$ , ranging from  $1300$  to  $8000 \text{ km s}^{-1}$ , showing that they belong in the category of quasars and active galaxies (White et al. 2000; Schneider et al. 2003). We also find that 13 are X-ray sources and 27 are infrared sources. In particular, SNUQSO J210931.9-353258 has been previously identified as a gamma-ray blazar source by Sowards-Emmerd et al. (2005), but without redshift identification. We now identify this object to be a quasar at  $z = 0.202$ .

The  $E(B - V)$  values in the direction of quasars/AGNs range from  $0.1$  to  $0.9$  with the median value at  $E(B - V) = 0.214$ . We examined whether there is a correlation between the Balmer decrement and the  $E(B - V)$  value. To do so, spectra are arranged according to the order of increasing  $E(B - V)$  value in Figure 2. The figure shows that there is a general tendency of weakening of  $H\beta$  flux with respect to  $H\alpha$  flux as the  $E(B - V)$  values increase. We have plotted the  $H\beta$  to  $H\alpha$  ratio versus  $E(B - V)$  and confirmed this general trend, but find a large scatter in the relation too. Detailed model-fitting of spectra and the observation during photometric nights may reduce the scatter, but it may not help much, since the large scatter could indicate that the line ratios of some of the quasars/AGNs do not reflect the simple case B recombination (e.g., Glickman et al. 2006; Soifer et al. 2004). The intrinsic scatter in this ratio due to dust absorption within quasars/AGNs and their host galaxies also complicates the interpretation.

The radio-to-optical ratios ( $R^*$ ) of the newly discovered quasars/AGNs range between  $0.1$  and  $282$  with the median value at  $1.9$ . The radio-to-optical flux ratio is defined to be the ratio of flux at the rest-frame  $6 \text{ cm}$  to  $0.44 \mu\text{m}$  (Stocke et al. 1992). The  $6\text{cm}$  flux is derived from the  $21\text{cm}$  flux assuming a power-law of  $f_\nu \sim \nu^{-0.46}$  (Ho & Ulvestad 2001), and applying a corresponding power-law  $K$ -correction in the form of  $K(z) = -2.5(\alpha + 1) \log(1 + z)$  where  $\alpha = -0.46$ . The  $0.44 \mu\text{m}$  flux is derived from the  $B$ -band apparent magnitude in Table 1, corrected for Galactic extinction (Schlegel et al. 1998), as well as for the  $K$ -correction derived from the SDSS quasar composite spectrum of Vanden Berk et al. (2001). We find six radio-loud quasars ( $R^* > 10$ ) which corresponds to  $16\%$  of our sample, excluding three AGNs. This number is slightly higher than the often-quoted value of  $10\%$  from more complete surveys at the magnitude range of our sample (e.g., Figure 18 in Ivezić et al. 2002; Hewett et al. 2001). The difference appears to be at least partially related to the radio selection of

---

Camera installed on the  $1.5\text{m}$  telescope at the Maidanak Observatory (Ko et al. 2007, in preparation). Application of this  $K$ -correction to the photographic  $R$ -band magnitude from USNO may result in a difference on the order of  $\sim 0.1 \text{ mag}$ .

our sample.

In Figure 3, we plot the  $R$ -band magnitude distribution of the newly discovered quasars/AGNs, before and after applying the extinction correction assuming the reddening map of Schlegel et al. (1998). Before applying the extinction correction, the distribution peaks at  $R \sim 16$  mag, with a wide tail toward  $R \sim 18$  mag, showing that our sample completeness is skewed toward the brighter magnitude of  $R < 16$  mag. After applying the extinction correction, many  $R > 16$  mag quasars/AGNs move toward the  $R < 16$  mag area, making our sample appear as if it were selected to be  $R \lesssim 16$  mag. Note that the Galactic extinctions,  $A_R$  and  $A_B$ , range from 0.22 to 2.57 mag and 0.25 to 4.04 mag, respectively, toward the quasars/AGNs.

Some of the quasars are found to be fairly bright. If USNO apparent magnitudes are accurate (see Section 3), SNUQSO J035657.03+425540.6 and SNUQSO J062355.21+001843.4 would have  $R \lesssim 14$  after Galactic extinction correction, making them two of the brightest quasars discovered to date.

The 40 quasars/AGNs are discovered over about  $2700 \text{ deg}^2$  of the sky, and therefore their surface number density is  $0.014 \text{ deg}^{-2}$  down to  $R \lesssim 16$  mag. We compare this number to the surface density of optically selected quasars/AGNs at high Galactic latitude from La Franca & Cristiani (1997), and also to the radio selected quasars from White et al. (2000). Assuming  $B - R \simeq 0.7$  mag for quasars (Becker et al. 2001), our effective magnitude cut of  $R < 16$  mag can be converted to  $B \lesssim 17$  mag. At that magnitude limit, La Franca & Cristiani (1997) find the surface number density of quasars to be roughly  $0.05 \text{ deg}^{-2}$  (See also Croom et al. 2004). On the other hand, White et al. (2000) find about 70 quasars at  $R \lesssim 16$  over  $2682 \text{ deg}^2$  which gives the surface density of  $0.026 \text{ deg}^{-2}$ . Our surface number density is nearly one half of the radio-selected sample of White et al. (2000). The major reason for the discrepancy is our preferential selection of lower redshift quasars/AGNs with the adopted  $J - K$  cut, which leads to the exclusion of about 50% of  $R < 16$  quasars at  $z \gtrsim 0.4$  (see Figure 8 in White et al. 2000). Also, a part of the discrepancy can be explained with the difference in the depth of the radio data (2.5 mJy versus our 1 mJy). The discrepancy in the surface number density from the optically selected sample can be explained by the radio selection as well as the reasons mentioned above. In any case, we expect that our sample is close to complete at the NVSS radio flux limit only for quasars at  $R < 16$  and  $z \lesssim 0.4$ .

Objects which are not classified as quasars are mostly Galactic objects, but some have featureless spectra similar to BL Lac objects. These objects will be discussed in a future work.

## 5. CONCLUSION

By combining the radio and NIR quasar selection algorithm, we have derived an algorithm which is efficient for selecting quasars with a minimal contamination rate. We applied this algorithm to search for quasars in low Galactic latitude regions which are crowded with stars. From the first two observing runs in 2006, we discovered 40 bright quasars/AGNs out of 88 candidates. The newly discovered quasars/AGNs will be useful for various astronomical studies such as the distribution of Galactic matter and the check of reddening maps, and the quasar host galaxy study using a nearby bright star as a guide star.

This work was supported by grant R01-2005-000-10610-0 from the Basic Research Program of the Korea Science and Engineering Foundation. This work uses a CCD camera purchased by a special research grant from the College of Natural Sciences, Seoul National University. We thank the staff at BOAO, especially Kang-Min Kim Byeong-Cheol Lee, and Youngbom Jeon for their professional aid during our observing runs, and the staff and scientists at the Maidanak Observatory, especially Rivkat Karimov and Mansur Ibrahimov for their assistance during the imaging observation. We also thank Patrick Hall, Luis C. Ho, Roc Cutri, and Alastair Edge for useful discussions.

Facilities: BOAO:1.8m, Maidanak:1.5m

## REFERENCES

- Adelman-McCarthy, J., et al. 2006, *ApJS*, 162, 38
- Barkhouse, W. A., & Hall, P. B. 2001, *AJ*, 121, 2843
- Becker, R. H., et al. 2001, *ApJS*, 135, 227
- Chiu, K., et al. 2007, *MNRAS*, 375, 1180
- Condon, J. J., et al. 1998, *AJ*, 115, 1693
- Croom, S. M., et al. 2004, *MNRAS*, 349, 1397
- Cutri, R. M., et al. 2000, in *The New Era of Wide-Field Astronomy*, ed. R. Clowes (San Francisco : ASP), 232
- Fan, X, Carilli, C. L., & Keating, B. 2006, *ARA&A*, 44, 415
- Glickman, E., Helfand, D. J., & White, R. L. 2006, *ApJ*, 640, 579
- Hagen. H.-J. et al. 1995, *A&AS*, 111, 195
- Hewett, P. C., Foltz, C. B., & Chaffee, F. H. 1995, *ApJ*, 109, 1498

- Hewett, P. C., Foltz, C. B., & Chaffee, F. H. 2001, *AJ*, 122, 518
- Ho, L. C., & Ulvestad, J. S. 2001, *ApJS*, 133, 77
- Ivezic, Z., et al. 2002, *AJ*, 124, 2364
- Kaspi, S., et al. 2000, *ApJ*, 533, 631
- Kim, K.-M., et al. 2003, *Publ. Korean Astron. Soc.* , 18, 81
- Kim, M., H. L. C., & Im, M. *ApJ*, 642, 702
- La Franca, F., Cristiani, S. 1997, *AJ*, 113, 1517
- Lee, I., et al. 2008, *ApJS*, 175, 116
- Maddox, N., & Hewett, P. C. 2006, *MNRAS*, 367, 717
- Monet, D., et al. 1998, *The USNO-A2.0 Catalogue* (U.S. Naval Observatory, Washington DC)
- Nelson, B., et al. 1998, in *AAS Meeting*, 193, 8104
- Rauch, M. 1998, *ARA&A*, 36, 267
- Richards, G. T., et al. 2004, *ApJS*, 155, 257
- Robin, A. C., Reyle, C., Derriere, S, & Picaud, S. 2003, *å*, 409, 523
- Savage, B., D., & Sembach K. R. 1996, *ARA&A*, 34, 279
- Schlegel, D. J., Finkbeiner, D. P., & Davis, M. 1998, *ApJ*, 500, 525
- Schmidt, M., 1963 *Nature*, 197, 1040S
- Schmidt, M., & Green, R. F. 1983, *ApJ*, 269, 352
- Schneider, D. P., et al. 2005, *AJ*, 130, 367
- Schneider, D. P., et al. 2003, *AJ*, 126, 2579
- Sembach, K. R., et al. *ApJS*, 146, 165
- Skrutskie, M. F., et al. 2006, *AJ*, 131, 1163
- Soifer, B. T., et al. 2004, *ApJS*, 154, 151
- Sowards-Emmerd, D., Romani, R. W., Michelson, P. F., Healey, S. E., & Nolan, P. L. 2005, *ApJ*, 626, 95
- Spagna, A. et al. 1996, *å*, 311, 758
- Sternberg, A. 2003, *Nature*, 421, 708
- Stocke, J. T., Morris, S. L., Weymann, R. J., & Foltz, C. B. 1992, *ApJ*, 396, 487
- Vanden Berk, D. E., et al. 2001, *AJ*, 122, 549

Veron-Cetty, M.-P., Veron, P. 2006, *A&A*, 455, 773

Weymann, R. J., Carswell, R. F., & Smith, M. G. 1981, *ARA&A*, 19 41

White, R. L., et al. 2000, *ApJS*, 126, 133

Table 1. Properties of the newly discovered quasars/AGNs.

ID	SNUQSO Name	R.A. (J2000)	Decl. (J2000)	$l$ (deg)	$b$ (deg)	$z$	$R$ (mag)	$B$ (mag)	$K$ (mag)	$J - K$ (mag)	$M_R$ (mag)	$F$ (mJy)	Ext. (mag)	$A_B$ (mag)	$A_R$ (mag)	Comm.
(1)	(2)	(3)	(4)	(5)	(6)	(7)	(8)	(9)	(10)	(11)	(12)	(13)	(14)	(15)	(16)	(17)
1	J010629.99+461935.1	01:06:29.99	46:19:35.1	125.64242	-16.46592	0.1243	16.3	18.0	12.81	1.78	-23.0	10.8	0.12	0.43	0.33	
2	J022540.43+583457.1	02:25:40.43	58:34:57.1	134.96545	-2.06997	0.0971	17.0	18.2	12.75	1.61	-23.9	8.5	0.95	4.04	2.57	IR
3	J035657.03+425540.6	03:56:57.03	42:55:40.6	155.29287	-7.99082	0.0659	15.0	16.1	11.08	2.17	-23.9	14.7	0.54	2.20	1.42	IR, X
4	J041239.56+582518.2	04:12:39.56	58:25:18.2	146.79854	5.20963	0.0675	16.0	17.1	12.26	1.69	-23.7	3.0	0.82	3.46	2.21	
5	J042533.12+344719.5	04:25:33.12	34:47:19.5	165.05205	-10.03833	0.0578	15.4	16.6	11.30	2.17	-22.5	5.8	0.30	1.18	0.79	X
6	J045458.67+694945.6	04:54:58.67	69:49:45.6	141.21285	16.18279	0.1401	15.2	15.8	12.10	2.23	-24.4	3.5	0.14	0.49	0.36	IR
7	J050322.13+592656.0	05:03:22.13	59:26:56.0	150.38249	10.78847	0.0963	17.3	19.0	12.18	2.19	-20.9	4.7	0.66	2.75	1.76	IR
8	J051148.53+282127.4	05:11:48.53	28:21:27.4	176.38036	-6.50323	0.1331	17.6	19.3	12.89	1.80	-23.4	19.0	0.73	3.02	1.93	
9	J051832.42+031609.4	05:18:32.42	03:16:09.4	198.84259	-18.92777	0.0572	15.6	17.1	12.64	1.86	-21.8	9.0	0.11	0.38	0.30	
10	J052807.06+054011.7	05:28:07.06	05:40:11.7	197.92783	-15.65704	0.1012	16.5	17.2	12.71	1.83	-22.9	28.1	0.35	1.45	0.96	IR
11	J052901.65+105709.8	05:29:01.65	10:57:09.8	193.36578	-12.75781	0.0764	15.8	16.6	12.84	1.56	-22.9	3.7	0.35	1.37	0.91	X
12	J053221.32+393922.1	05:32:21.32	39:39:22.1	169.46582	3.39566	0.0720	18.3	17.8	12.51	1.55	-21.3	2.8	0.72	3.07	1.97	IR
13	J054706.34+442026.7	05:47:06.34	44:20:26.7	166.90147	8.18474	0.1190	17.0	16.8	13.23	1.60	-22.7	4.0	0.34	1.35	0.90	IR
14	J054854.50+363250.6	05:48:54.50	36:32:50.6	173.83374	4.52368	0.0745	17.2	19.1	13.58	1.54	-22.4	5.8	0.68	2.86	1.83	IR
15	J055447.25+662043.8	05:54:47.25	66:20:43.8	147.27239	19.28736	0.1859	14.5	14.6	11.41	2.17	-25.8	5.6	0.16	0.59	0.43	X
16	J060040.11+000618.6	06:00:40.11	00:06:18.6	206.97350	-11.22760	0.1147	17.6	19.0	11.75	2.19	-23.2	212.7	0.74	3.20	2.04	IR
17	J061713.50+285138.3	06:17:13.50	28:51:38.3	183.48294	5.97938	0.1036	16.4	17.3	12.01	2.04	-23.9	10.7	0.68	2.82	1.81	IR,X
18	J061717.30+430056.0	06:17:17.30	43:00:56.0	170.68829	12.38432	0.2067	17.1	17.3	13.36	1.73	-23.5	20.9	0.15	0.54	0.40	IR
19	J062355.21+001843.4	06:23:55.21	00:18:43.4	209.50422	-5.97636	0.0940	14.8	15.4	11.09	1.92	-25.2	46.7	0.65	2.68	1.72	IR
20	J063100.52+503046.2	06:31:00.52	50:30:46.2	164.56062	17.54972	0.1805	16.8	16.7	13.08	1.92	-23.4	2.7	0.13	0.45	0.34	IR
21	J063652.52-081048.6	06:36:52.52	-08:10:48.6	218.59605	-6.93935	0.2328	15.7	15.6	13.23	1.64	-26.1	2.7	0.48	2.00	1.30	X
22	J064139.37+451002.0	06:41:39.37	45:10:02.0	170.45824	17.25334	0.2973	16.3	16.4	12.84	2.08	-25.1	24.3	0.11	0.39	0.30	X
23	J064410.86+354644.6	06:44:10.86	35:46:44.6	179.66110	14.10731	0.0772	14.3	15.9	11.83	1.80	-23.9	53.7	0.16	0.60	0.43	
24	J064856.41+352206.6	06:48:56.41	35:22:06.6	180.44495	14.83466	0.1193	15.8	16.2	12.90	1.75	-23.4	4.1	0.12	0.42	0.32	X
25	J071014.55+131535.2	07:10:14.55	13:15:35.2	203.12061	10.11274	0.1411	15.8	16.2	12.32	2.11	-23.7	6.7	0.08	0.25	0.22	IR
26	J071215.61+153930.3	07:12:15.61	15:39:30.3	201.12942	11.58509	0.1656	15.3	16.1	12.42	1.79	-25.0	4.1	0.23	0.99	0.68	X
27	J071645.09+002749.8	07:16:45.09	00:27:49.8	215.41248	5.84219	0.0519	15.1	16.3	12.13	1.56	-22.3	4.1	0.21	0.79	0.55	IR
28	J073939.54-094456.2	07:39:39.54	-09:44:56.2	227.16980	6.08370	0.1007	15.7	16.1	12.20	2.11	-23.2	15.2	0.17	0.66	0.47	IR
29	J170631.57-064638.6	17:06:31.57	-06:46:38.6	14.02261	19.67993	0.1046	16.5	17.8	13.03	1.66	-23.5	7.2	0.55	2.34	1.45	IR, X
30	J175925.57+171513.5	17:59:25.57	17:15:13.5	43.04643	19.05558	0.1454	16.0	16.8	13.11	1.81	-23.6	14.3	0.10	0.44	0.27	X
31	J180508.94+124253.9	18:05:08.94	12:42:53.9	39.30022	15.93342	0.1707	16.7	17.8	13.44	1.82	-23.6	12.8	0.22	0.97	0.60	IR
32	J193013.80+341049.5	19:30:13.80	34:10:49.5	67.57943	7.59368	0.0616	15.9	17.7	11.81	2.32	-21.9	3.9	0.19	0.84	0.52	IR
33	J193347.16+325426.0	19:33:47.16	32:54:26.0	66.79822	6.34119	0.0565	14.5	15.5	11.34	1.70	-23.3	4.0	0.27	1.16	0.72	IR, X

Table 1—Continued

ID	SNUQSO Name	R.A. (J2000)	Decl. (J2000)	$l$ (deg)	$b$ (deg)	$z$	$R$ (mag)	$B$ (mag)	$K$ (mag)	$J - K$ (mag)	$M_R$ (mag)	$F$ (mJy)	Ext. (mag)	$A_B$ (mag)	$A_R$ (mag)	<i>Comm.</i>
(1)	(2)	(3)	(4)	(5)	(6)	(7)	(8)	(9)	(10)	(11)	(12)	(13)	(14)	(15)	(16)	(17)
34	J193521.19+531411.9	19:35:21.19	53:14:11.9	85.40431	15.29883	0.2478	15.8	16.5	13.15	1.54	-25.1	10.4	0.11	0.50	0.31	IR
35	J203332.03+214622.3	20:33:32.03	21:46:22.3	64.38411	-10.77715	0.1735	16.2	17.7	13.05	1.74	-23.9	340.4	0.14	0.59	0.36	
36	J210931.88+353257.6	21:09:31.88	35:32:57.6	80.28167	-8.35288	0.2023	14.7	15.7	13.03	1.49	-25.8	1195.7	0.16	0.61	0.38	IR, X, GB
37	J212235.46+273846.5	21:22:35.46	27:38:46.5	76.26527	-15.75300	0.0909	16.0	17.2	13.23	1.52	-22.6	5.6	0.13	0.59	0.36	IR
38	J212756.45+271905.8	21:27:56.45	27:19:05.8	76.86721	-16.84005	0.1974	16.3	18.3	12.64	2.21	-24.1	6.4	0.12	0.50	0.31	IR
39	J222719.04+400550.2	22:27:19.04	40:05:50.2	95.18443	-14.88447	0.0659	15.6	16.9	11.91	2.19	-22.2	6.9	0.15	0.63	0.39	IR
40	J230329.93+453740.4	23:03:29.93	45:37:40.4	103.90851	-13.21915	0.3007	16.5	17.1	13.27	1.89	-25.6	5.0	0.35	1.40	0.93	IR

<sup>(8)–(10)</sup>  $R$ ,  $B$ , and  $K$ -band apparent magnitudes, not corrected for Galactic extinction.

<sup>(11)</sup>  $J - K$  color, not corrected for Galactic extinction.

<sup>(12)</sup>  $R$ -band absolute magnitude, corrected for Galactic extinction

<sup>(13)</sup> Flux at 1.4  $GHz$  from NVSS.

<sup>(14)</sup> Reddening parameter,  $E(B - V)$

<sup>(15),(16)</sup> Extinction at  $B$  and  $R$ -bands in magnitude unit, respectively.  $B$ -band extinction is calculated using  $A_B = 3.91 E(B - V)$  for USNO magnitudes, and  $A_B = 4.3 E(B - V)$  for the Maidanak data. For  $A_R$ , we used  $A_R = 2.93 E(B - V)$  for both cases, since the difference in the extinction correction arising from a small discrepancy in conversion factor is less than 0.01 mag between USNO-II  $R$  magnitude and the Maidanak  $R$  magnitude.

<sup>(17)</sup> Comments. ‘X’ stands for X-ray source, and ‘GB’ for Gamma-ray Blazar Candidate.

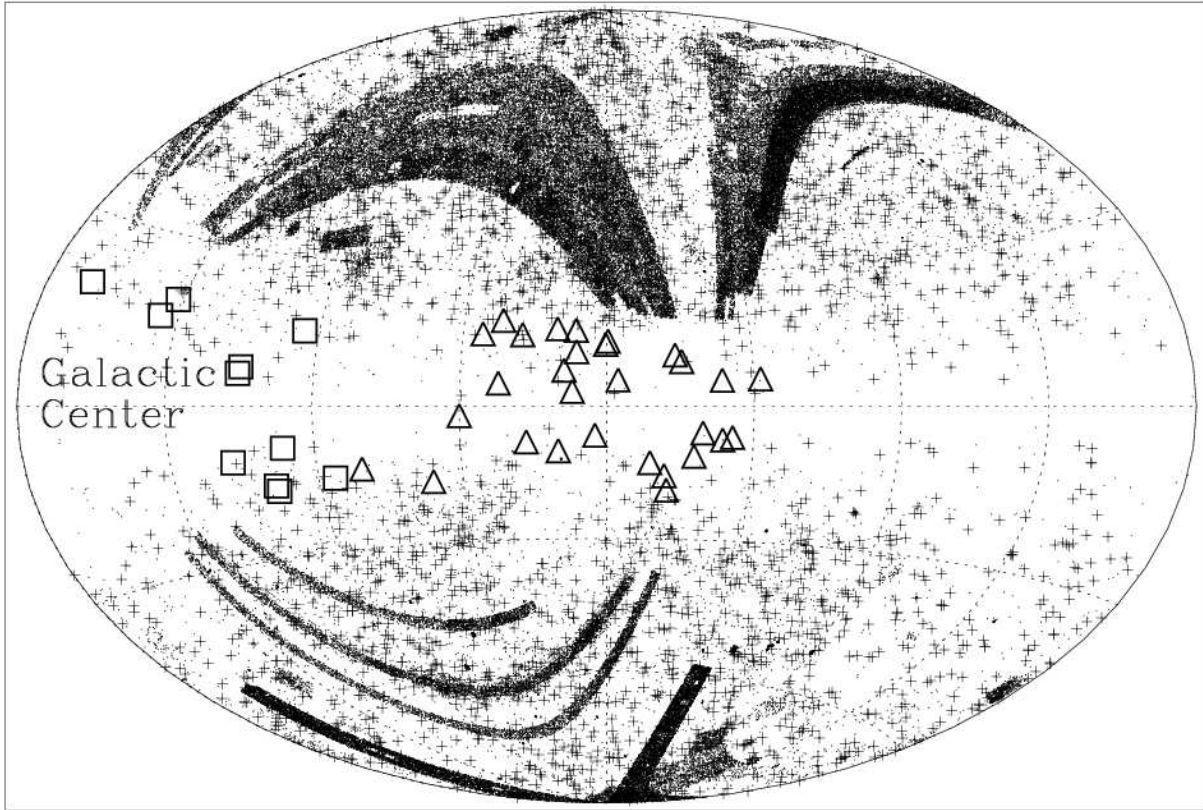


Fig. 1.— Distribution of quasars and AGNs in the sky, plotted in Galactic coordinates. Small dots represent the quasars/AGNs brighter than  $V < 23$  mag discovered to date, while crosses represent quasars/AGNs brighter than  $V = 17$  mag. Note a gap in the distribution between the northern and southern Galactic hemispheres. The newly discovered quasars are marked with squares (from 2006 June run) and triangles (from 2006 December run). **[High quality image is available on electronic journal]**

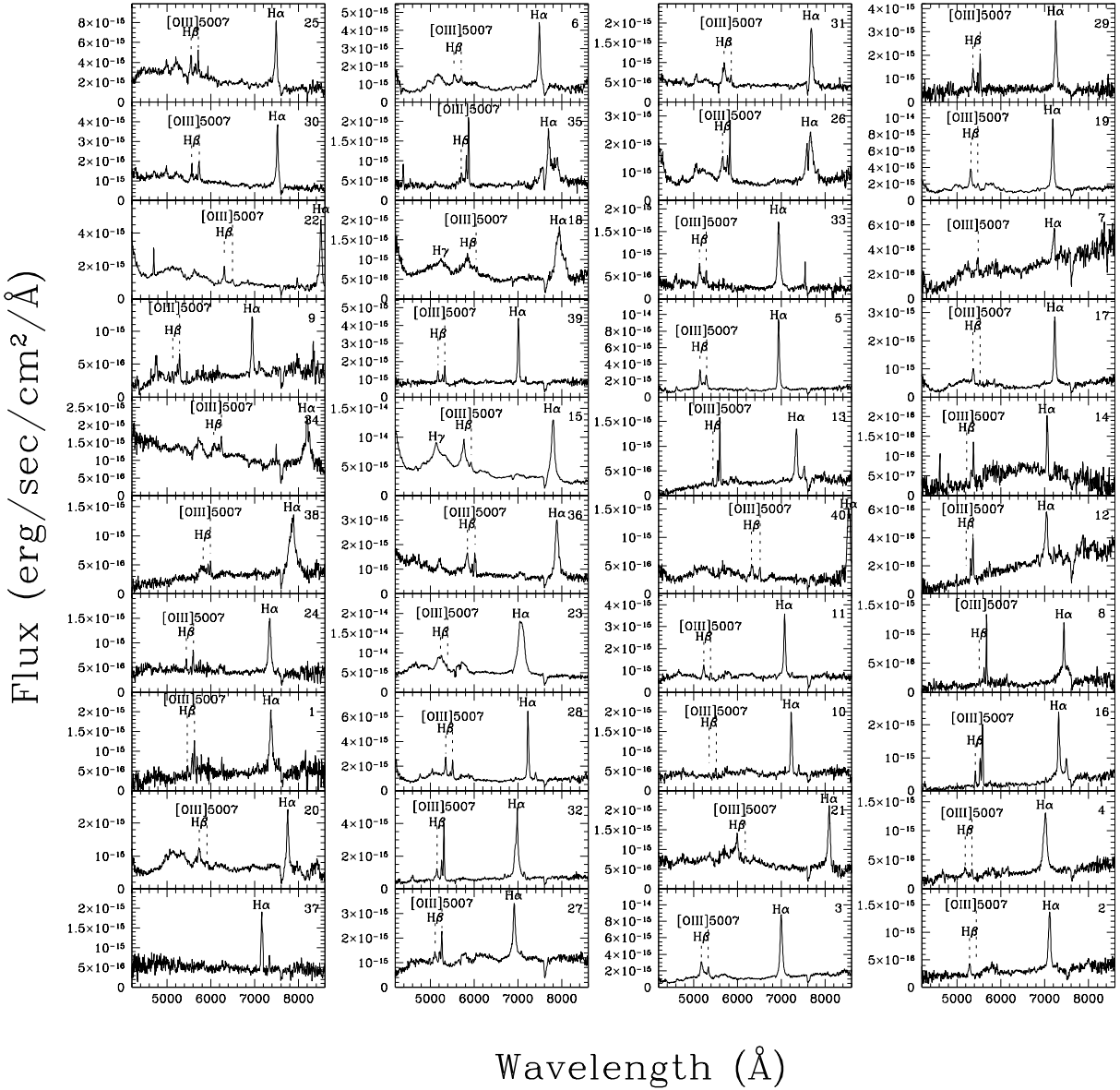


Fig. 2.— Optical spectra of the newly discovered quasars, plotted in the order of increasing  $E(B - V)$  values. The  $E(B - V)$  values increase from top to bottom, left to right. Broad Balmer emission lines and [O III] lines are visible for most of the quasars except for those at the location where the Galactic extinction is high.

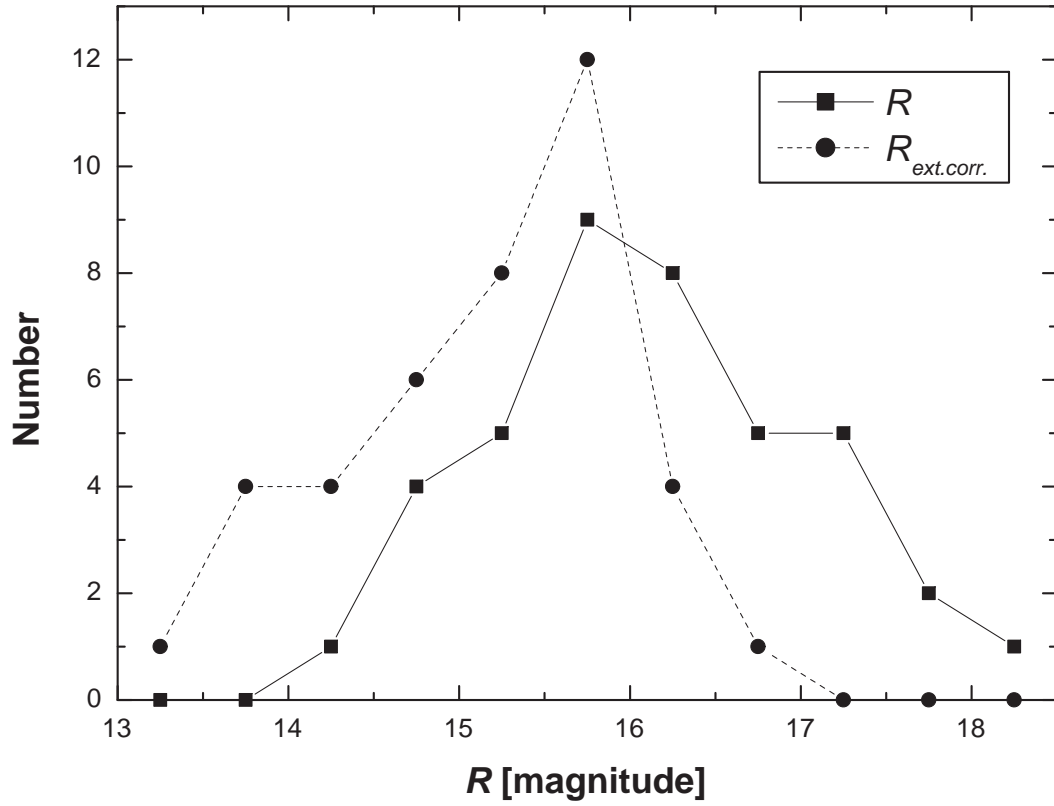


Fig. 3.—  $R$ -band apparent magnitude of the newly discovered quasars before (squares and solid line) and after (circles and dashed line) the extinction correction. From this figure and the analysis of the surface number density (see text), we find that our sample has an effective optical magnitude cut of  $R < 16$  mag.